

On the choice of beam polarization in $e^+e^- \rightarrow ZZ/Z\gamma$ and anomalous triple gauge-boson couplings

Rafiqul Rahaman^{a,1}, Ritesh K. Singh^{b,1}

¹Department of Physical Sciences, Indian Institute of Science Education and Research Kolkata, Mohanpur, 741246, India

Compiled: Tuesday 21st March, 2017 at 00:25

Abstract The anomalous trilinear gauge couplings of Z and γ are studied in $e^+e^- \rightarrow ZZ/Z\gamma$ with longitudinal beam polarizations using a complete set of polarization asymmetries for Z boson. We quantify the goodness of the beam polarization in terms of the likelihood and find best choice of e^- and e^+ polarizations to be $(+0.16, -0.16)$, $(+0.09, -0.10)$ and $(+0.12, -0.12)$ for ZZ , $Z\gamma$ and combined processes, respectively. Simultaneous limits on anomalous couplings are obtained for these choices of beam polarizations using Markov-Chain-Monte-Carlo (MCMC) for an e^+e^- collider running at $\sqrt{s} = 500$ GeV and $\mathcal{L} = 100 \text{ fb}^{-1}$. We find the simultaneous limits for these beam polarizations to be comparable with each other and also comparable with the unpolarized beam case.

1 Introduction

Gauge boson sector in the Standard Model (SM) remains uncharted even after the discovery of Higgs boson [1] at LHC. Gauge boson self couplings (trilinear and quartic), gauge boson couplings to Higgs, Higgs self couplings, which are the key area to understand the Electro Weak Symmetry Breaking (EWSB), have no precise measurements and need serious attention. Future International Linear Collider (ILC) [2–4] will be a precision testing machine [5] which will have the possibility of having polarized initial beams. Two type of polarization, namely longitudinal and transverse, for both initial beams (e^- and e^+) will play an important role in precise measurement of various parameters, like coupling among gauge boson, Higgs coupling to top quark, Higgs coupling to gauge boson. Beam polarization has the ability to enhance the relevant signal to background ratio along with the sensitivity of observables [5–9]. It can also be used to

separate CP-violating couplings from CP-conserving one [5, 10–19] if CP-violation is present in the nature. These potentials of the beam polarizations has been explored, for example, to study τ polarization [11], top quark polarization [20] and its anomalous couplings [21], littlest Higgs model [22], WWV couplings [6, 7, 23], Higgs couplings to gauge bosons [24–27].

Here we use beam polarizations (longitudinal only) to study anomalous trilinear gauge boson self couplings in the neutral sector using the complete set of polarization observables of Z boson [28–30] in the process $e^+e^- \rightarrow ZZ/Z\gamma$. The anomalous couplings among neutral gauge boson have been studied earlier with unpolarized beam in [31–38] as well as with polarized beams [15–17, 19, 39–44]. Some of these studies have used a given beam polarizations to enhance sensitivity of observables while others have used two different set of beam polarization to construct observables. We follow the former method and quantify the likelihood based goodness of the choice of beam polarizations.

For the process of interest the anomalous triple gauge boson couplings is given by the Lagrangian [28, 40],

$$\begin{aligned} \mathcal{L} = \frac{g_e}{M_Z^2} \Bigg[& [f_4^Z(\partial_\mu Z^{\mu\beta}) - f_4^\gamma(\partial_\mu F^{\mu\beta})] Z_\alpha (\partial^\alpha Z_\beta) \\ & + [f_5^\gamma(\partial^\sigma F_{\sigma\mu}) + f_5^Z(\partial^\sigma Z_{\sigma\mu})] \tilde{Z}^{\mu\beta} Z_\beta \\ & - [h_1^\gamma(\partial^\sigma F_{\sigma\mu}) + h_1^Z(\partial^\sigma Z_{\sigma\mu})] Z_\beta F^{\mu\beta} \\ & - [h_3^\gamma(\partial_\sigma F^{\sigma\rho}) + h_3^Z(\partial_\sigma Z^{\sigma\rho})] Z^\alpha \tilde{F}_{\rho\alpha} \Bigg]. \end{aligned} \quad (1)$$

The coupling f_i^V ’s appear in the ZZ process while h_i^V ’s appear in $Z\gamma$ process. Among these couplings f_4^V and h_1^V are CP -odd while others are CP -even. These anomalous couplings have been recently probed at LHC [45, 46]. The available best limit from LHC are $|f_i^V| \sim 3 \times 10^{-3}$ [45] and $|h_i^V| \sim 9 \times 10^{-4}$ [46].

^aemail:rr13rs033@iiserkol.ac.in

^bemail:ritesh.singh@iiserkol.ac.in

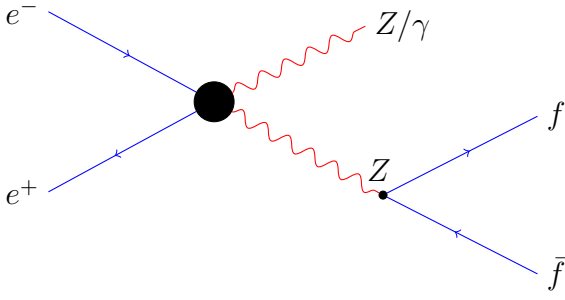


Fig. 1 Feynman diagram for production of Z boson and its decay to a pair of fermions.

Rest of the paper is organized as follows. In [section 2](#) we discuss basic formulations and the Z boson polarization observables. In [section 3](#) we study beam polarization dependence of sensitivity and likelihood. We define a *measure of goodness* for the choice of beam polarizations and study ZZ/Z γ processes to obtain the best choices. The best simultaneous limits are presented for a set of beam polarizations. We conclude in [section 4](#).

2 Beam polarization and polarization observables

The polarization density matrices for e^- and e^+ beams are given by,

$$P_{e^-}(\lambda_{e^-}, \lambda'_{e^-}) = \frac{1}{2} \begin{bmatrix} (1 + \eta_3) & \eta_T \\ \eta_T & (1 - \eta_3) \end{bmatrix} \quad \text{and} \quad (2)$$

$$P_{e^+}(\lambda_{e^+}, \lambda'_{e^+}) = \frac{1}{2} \begin{bmatrix} (1 + \xi_3) & \xi_T e^{-i\delta} \\ \xi_T e^{i\delta} & (1 - \xi_3) \end{bmatrix}, \quad (3)$$

where η_3 and η_T (ξ_3 and ξ_T) are longitudinal and transverse polarization of e^- (e^+) with δ being the azimuthal angle between two transverse polarizations. The positive x -axis is taken along the transverse polarization of e^- and positive z -axis along its momentum.

The density matrix for the production of Z boson in the above process (Fig. 1) would be,

$$\rho(\lambda_Z, \lambda'_Z) = \sum_{\lambda_{e^-}, \lambda'_{e^-}, \lambda_{e^+}, \lambda'_{e^+}} \mathcal{M}^\dagger(\lambda'_{e^-}, \lambda'_{e^+}, \lambda'_Z) \times \mathcal{M}(\lambda_{e^-}, \lambda_{e^+}, \lambda_Z) \times P_{e^-}(\lambda_{e^-}, \lambda'_{e^-}) \times P_{e^+}(\lambda_{e^+}, \lambda'_{e^+}). \quad (4)$$

We note that different helicities can take following values:

$$\lambda_Z, \lambda'_Z \in \{-1, 0, 1\} \text{ and } \lambda_{e^\pm}, \lambda'_{e^\pm} \in \{-1, 1\}. \quad (5)$$

For the present work we restrict ourselves only to the longitudinal beam polarizations, i.e. $\eta_T = 0 = \xi_T$. With chosen beam polarizations we construct the complete set of 8 polarization observables for the Z boson along with total cross-section in the processes $e^+e^- \rightarrow ZZ/Z\gamma$. These polarization observables can be obtained analytically from the production process as well as from asymmetries constructed

from decay distribution of the particle. The polarization observables consist of a 3 component vector polarization $\mathbf{P} \equiv (P_x, P_y, P_z)$ and a traceless symmetric rank-2 tensor T_{ij} ($i, j = x, y, z$) with 5 independent component T_{xy} , T_{xz} , T_{yz} , $T_{xx} - T_{yy}$ and T_{zz} . The asymmetries in the collider or in a Monte Carlo event generator corresponding to P_i 's and T_{ij} 's are $\{A_x, A_y, A_z\}$ and $\{A_{xy}, A_{xz}, A_{yz}, A_{x^2-y^2}, A_{zz}\}$, respectively. The asymmetries A_z, A_{xz}, A_{yz} are zero in SM and even with polarized beam in both the processes owing to forward backward symmetry of produced Z in these processes. To make these asymmetries non-zero we redefine the polarization observables $\mathcal{O} \in \{P_z, T_{xz}, T_{yz}\}$ as:

$$\mathcal{O} \rightarrow \tilde{\mathcal{O}} = \frac{1}{\sigma_Z} \left[\int_0^{c_{\theta_0}} \text{Comb}(\mathcal{O}, \sigma(\lambda, \lambda')) dc_{\theta_Z} - \int_{-c_{\theta_0}}^0 \text{Comb}(\mathcal{O}, \sigma(\lambda, \lambda')) dc_{\theta_Z} \right], \quad (6)$$

where c_{θ_0} is the beam pipe cut and $\text{Comb}(\mathcal{O}, \sigma(\lambda, \lambda'))$ is the combination of production density matrix corresponding the polarization observable \mathcal{O} (see Ref. [28]). For example, with $\mathcal{O} = P_z$ one has

$$\text{Comb}(P_z, \sigma(\lambda, \lambda')) = \rho(+1, +1) - \rho(-1, -1)$$

and the corresponding modified polarization is given by

$$\tilde{P}_z = \frac{1}{\sigma_Z} \left[\int_0^{c_{\theta_0}} \left[\rho(+1, +1) - \rho(-1, -1) \right] dc_{\theta_Z} - \int_{-c_{\theta_0}}^0 \left[\rho(+1, +1) - \rho(-1, -1) \right] dc_{\theta_Z} \right]. \quad (7)$$

The asymmetries \tilde{A}_z corresponding to the modified polarization \tilde{P}_z is given by:

$$\tilde{A}_z \equiv \frac{1}{\sigma} \left(\sigma(c_{\theta_Z} \times c_{\theta_f} > 0) - \sigma(c_{\theta_Z} \times c_{\theta_f} < 0) \right). \quad (8)$$

Similarly A_{xz} and A_{yz} related to T_{xz} and T_{yz} are modified as

$$\begin{aligned} \tilde{A}_{xz} &\equiv \frac{1}{\sigma} \left(\sigma(c_{\theta_Z} \times c_{\theta_f} c_{\phi_f} > 0) - \sigma(c_{\theta_Z} \times c_{\theta_f} c_{\phi_f} < 0) \right), \\ \tilde{A}_{yz} &\equiv \frac{1}{\sigma} \left(\sigma(c_{\theta_Z} \times c_{\theta_f} s_{\phi_f} > 0) - \sigma(c_{\theta_Z} \times c_{\theta_f} s_{\phi_f} < 0) \right). \end{aligned} \quad (9)$$

Redefining these asymmetries increases the total number of the non-vanishing observables to put simultaneous limit on the anomalous coupling and we expect limits tighter than reported earlier in Ref. [28].

The total cross-section (or total number of events) of a process plays an important role determining the sensitivity and the limits on the anomalous couplings. Tighter limit on the anomalous couplings can be obtained if the cross-section can be enhanced. Beam polarization can enhance the cross-section and hence it is important to see how it depends on beam polarization. Fig. 2 shows the dependence

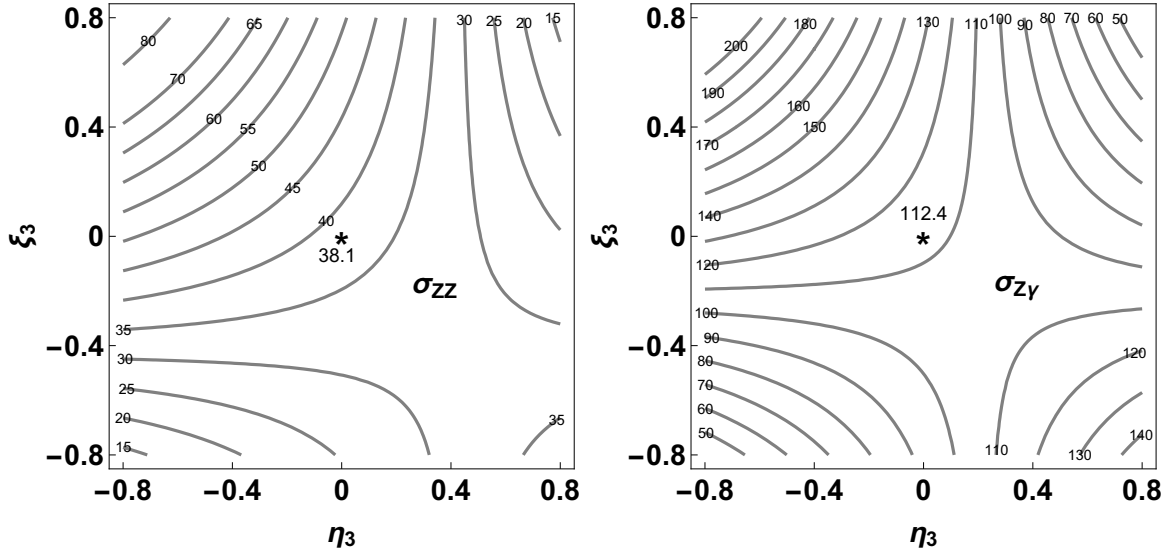


Fig. 2 The SM cross-section (in fb) for the process $e^+e^- \rightarrow ZZ/Z\gamma$ as a function of longitudinal beam polarizations η_3 (for e^-) and ξ_3 (for e^+) at $\sqrt{s} = 500$ GeV.

of cross-sections σ_{ZZ} and $\sigma_{Z\gamma}$ on longitudinal beam polarizations η_3 and ξ_3 at $\sqrt{s} = 500$ GeV. The asterisk mark on the middle of the plots represents the unpolarized case. We notice that cross-section in both the processes are larger for negative value of η_3 and positive value of ξ_3 . Sensitivity on cross section is expected to be high in the left-top corner of the $\eta_3 - \xi_3$ plane. This would convince us to set beam polarizations at the left-top corner for analysis. But cross-section is not the only observable, the asymmetries have different behavior on beam polarizations. For example, A_x peaks at the right bottom corner, i.e. opposite behavior compared to cross-section, while A_z has similar dependence as cross-section on the beam polarizations in both the processes. Processes involving W^\pm are also expected to have higher cross-section at the left-top corner of $\eta_3 - \xi_3$ plane as W couple to the left chiral electron. Anomalous couplings are expected to change the dependence of all the observables, including cross-section, on the beam polarizations. To explore this we study the effect of beam polarizations on sensitivity of cross-section and other observables to anomalous couplings in the next section.

3 Sensitivity, likelihood and the choice of beam polarizations

Sensitivity of an observables \mathcal{O} depending on anomalous couplings \mathbf{f} with a given beam polarizations η_3 and ξ_3 is given by,

$$\mathcal{S}(\mathcal{O}(\mathbf{f}, \eta_3, \xi_3)) = \frac{|\mathcal{O}(\mathbf{f}, \eta_3, \xi_3) - \mathcal{O}(\mathbf{0}, \eta_3, \xi_3)|}{|\delta \mathcal{O}(\eta_3, \xi_3)|}, \quad (10)$$

where $\delta \mathcal{O} = \sqrt{(\delta \mathcal{O}_{stat.})^2 + (\delta \mathcal{O}_{sys.})^2}$ is the estimated error in \mathcal{O} . The estimated error to cross-section would be,

$$\delta \sigma(\eta_3, \xi_3) = \sqrt{\frac{\sigma(\eta_3, \xi_3)}{\mathcal{L}} + \epsilon_\sigma^2 \sigma(\eta_3, \xi_3)^2}, \quad (11)$$

where as the estimated error to asymmetries would be,

$$\delta A(\eta_3, \xi_3) = \sqrt{\frac{1 - A(\eta_3, \xi_3)^2}{\mathcal{L} \sigma(\eta_3, \xi_3)} + \epsilon_A^2}. \quad (12)$$

Here \mathcal{L} is the integrated luminosity, ϵ_σ and ϵ_A are the systematic fractional error in cross-section and asymmetries respectively. In these analysis we take $\mathcal{L} = 100 \text{ fb}^{-1}$, $\epsilon_\sigma = 0.02$ and $\epsilon_A = 0.01$ as a benchmark.

We study the sensitivity of all the observable and their dependence on beam polarizations at $\sqrt{s} = 500$ GeV. Choosing a benchmark value for anomalous couplings to be

$$\mathbf{f} = \{f_4^Y, f_4^Z, f_5^Y, f_5^Z\} = \{+3, +3, +3, +3\} \times 10^{-3},$$

we show the sensitivities for σ , A_{xy} and \tilde{A}_{yz} in Fig. 3 as a function of beam polarizations. The sensitivities for cross-section and \tilde{A}_{yz} peak at the left top corner of the plots. For A_{xy} sensitivity peaks at the right bottom corner it is not much smaller in the left-top corner either. The sensitivities of all other asymmetries (not shown here) except \tilde{A}_z peaks at the left top corner although the exact dependence on beam polarization may differ. Thus, the combined sensitivity of all the observables is high on the left top corner of the polarization plane making $(\eta_3, \xi_3) = (-0.8, +0.8)$ the best choice for the chosen benchmark coupling. This best choice, however, strongly depend upon the values of the anomalous couplings. We note that the best choice of the beam polarization

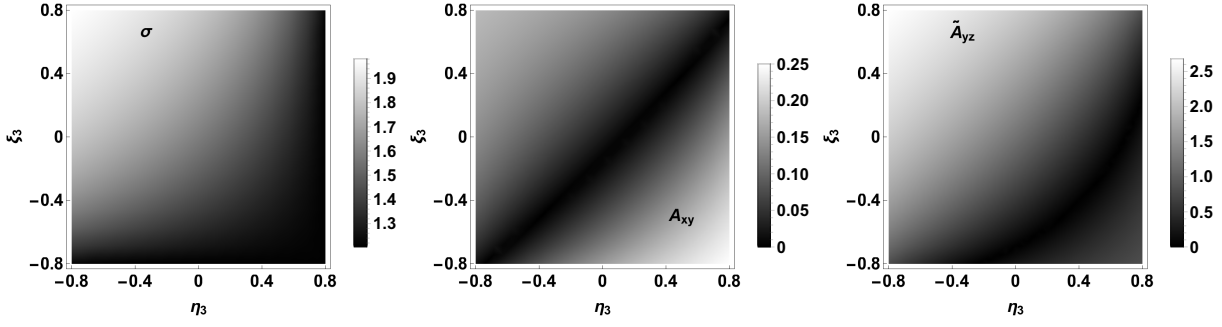


Fig. 3 Effect of beam polarizations on sensitivity of cross-section σ , A_{xy} and \tilde{A}_{yz} in the process $e^+e^- \rightarrow ZZ$ for anomalous couplings $\mathbf{f} = \{+3, +3, +3, +3\} \times 10^{-3}$ at $\sqrt{s} = 500$ GeV and $\mathcal{L} = 100 \text{ fb}^{-1}$.

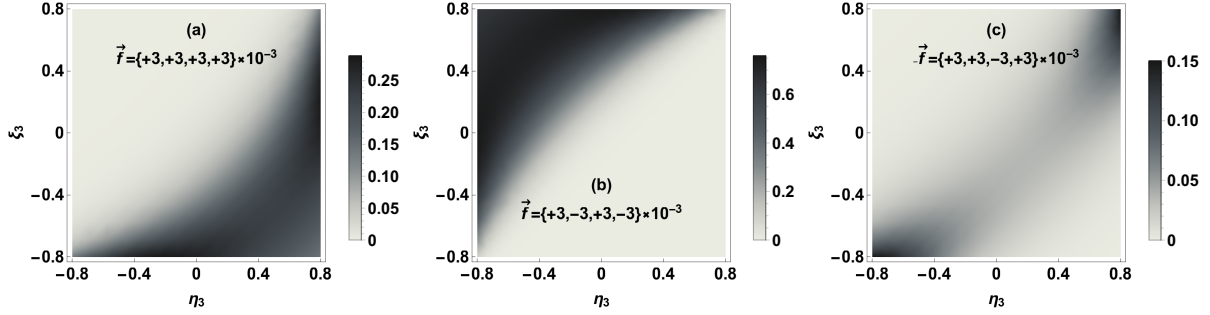


Fig. 4 Likelihood $L(\{\mathcal{O}\}, \mathbf{f}; \eta_3, \xi_3)$ for three different benchmark anomalous couplings at $\sqrt{s} = 500$ GeV and $\mathcal{L} = 100 \text{ fb}^{-1}$ in ZZ process.

is mainly decided by the behavior of the cross-section because most of the asymmetries also have similar dependence on the beam polarizations. This, however, does not mean that cross-section provides best sensitivity or the limits. For example, in Fig. 3 we can see that \tilde{A}_{yz} has better sensitivity than the cross-section. For the $Z\gamma$ process with for the benchmark point

$$\mathbf{h} = \{h_1^\gamma, h_1^Z, h_3^\gamma, h_3^Z\} = \{+3, +3, +3, +3\} \times 10^{-3}$$

one obtains similar conclusions: Sensitivities of all observables peak at left top corner of $\eta_3 - \xi_3$ plane (not shown) except for \tilde{A}_z .

For a complete analysis we need to use all the observable simultaneously. To this end we define a likelihood function considering the set of all the observables depending on anomalous coupling \mathbf{f} as,

$$L(\{\mathcal{O}\}, \mathbf{f}; \eta_3, \xi_3) = \exp \left[-\frac{1}{2} \sum_i \mathcal{S}(\mathcal{O}_i(\mathbf{f}, \eta_3, \xi_3))^2 \right], \quad (13)$$

i runs over the set of observables in a process. Maximum sensitivity of observables requires the likelihood to be minimum. The likelihood defined here is proportional to the p -value and hence best choice of beam polarizations comes from the *minimum* likelihood or maximum distinguishability.

The beam polarization dependence of the likelihood for the ZZ process at the above chosen anomalous couplings is given in Fig. 4(a). The minimum of the likelihood falls

in the left top corner of the $\eta_3 - \xi_3$ plane as expected as most of the observables has higher sensitivity at this corner. For different anomalous couplings the minimum likelihood changes its position in the $\eta_3 - \xi_3$ plane. We have checked the likelihood for 16 different corner of

$$\mathbf{f}_{\pm\pm\pm\pm} = \{\pm 3, \pm 3, \pm 3, \pm 3\} \times 10^{-3}$$

and they have different dependence on η_3, ξ_3 . Here we present likelihood for three different choice of anomalous couplings in Fig. 4. In Fig. 4(b), the minimum of the likelihood falls in the right bottom corner where most of the observables have higher sensitivity. In Fig. 4(c) low likelihood falls in both the diagonal corner in $\eta_3 - \xi_3$ plane. This is because some of the observables prefers left-top corner while others prefers right-bottom corner of the polarization plane for higher sensitivity. We have the similar behavior for the likelihood in the $Z\gamma$ process as well.

As the anomalous couplings change, the minimum likelihood region changes accordingly and hence the best choice of beam polarizations. So the best choice for the beam polarizations depends on the new physics in the process. If one knows the new physics one could tune the beam polarizations to have the best sensitivity for the analysis. But in order to have a suitable choice of beam polarizations irrespective of the possible new physics one needs to minimize the likelihood averaged over all the anomalous couplings. The beam polarizations with the minimum averaged likelihood is expected to be the average best choice for any new physics in

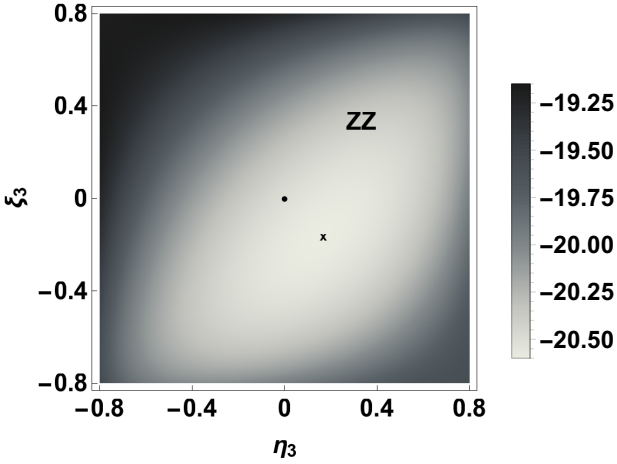


Fig. 5 The log of average likelihood, $\log[L(V_f, \{\mathcal{O}\}; \eta_3, \xi_3)]$ as a function of beam polarization is shown for the ZZ process at $\sqrt{s} = 500$ GeV and $\mathcal{L} = 100 \text{ fb}^{-1}$. The dot at the center is the (0,0) point while cross mark at $P_{ZZ} = (+0.16, -0.16)$ is the minimum likelihood point and hence the best choice of beam polarization for ZZ process.

the process. The likelihood function averaged over a volume in parameter space would be define as,

$$L(V_f, \{\mathcal{O}\}; \eta_3, \xi_3) = \int_{V_f} L(\{\mathcal{O}\}, \mathbf{f}; \eta_3, \xi_3) d\mathbf{f}, \quad (14)$$

where V_f is a volume in the parameter space (\mathbf{f}). Here we choose the volume to be a hypercube in the 4 dimensional parameter space with sides equals 2×0.01 (much larger than the available limits on them) in both the processes. Contribution to the average likelihood from the region outside this volume is negligible.

The averaged likelihood $L(V_f, \{\mathcal{O}\}; \eta_3, \xi_3)$ in the ZZ process as a function of beam polarization is shown in Fig. 5 on log-scale. The dot on the middle of the plot represents the unpolarized case and the cross mark at $P_{ZZ} = (+0.16, -0.16)$ represents the minimum averaged likelihood point i.e., the best choice of beam polarizations. This choice is not much far away from the unpolarized case. The unpolarized point, the best point and the points near them have same order of average likelihood and expected to give similar limits on anomalous couplings. To explore this we estimate simultaneous limits using Markov-Chain-Monte-Carlo (MCMC) method at P_{ZZ} , unpolarized beam and few other benchmark choice of beam polarization. The limits thus obtained on the anomalous couplings for the ZZ process are listed in Table 1. We note that the limits for the best choice of polarizations (P_{ZZ}) are best but comparable to other nearby benchmark beam polarization including the unpolarized beams. This is due to the average likelihood is comparable for these cases. We also note that the limits for unpolarized case in Table 1 are better than the ones reported in Ref. [28], when adjusted for the systematic errors. This improvement we get here is due to inclusion of three new non-vanishing asymmetries \tilde{A}_z ,

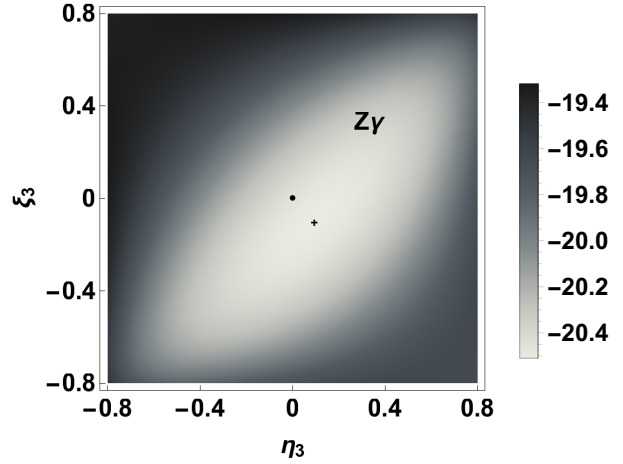


Fig. 6 Same as Figure 5 but for the $Z\gamma$ process. The plus mark at $P_{Z\gamma} = (+0.09, -0.10)$ is the lowest likelihood point and hence the best choice of beam polarization for $Z\gamma$ process.

\tilde{A}_{xz} and \tilde{A}_{yz} . Of these, \tilde{A}_{xz} has linear dependence on $f_5^{\gamma,Z}$ with larger sensitivity to f_5^Z leading to about 30% improvement in the limit. Similarly, the CP -odd asymmetry \tilde{A}_{yz} has linear dependence on $f_4^{\gamma,Z}$ with larger sensitivity to f_4^Z and this again leads to about 30% improvement in the corresponding limit. The asymmetry \tilde{A}_z has quadratic dependence on all four parameters and has too poor sensitivity for all of them to be useful.

We do similar analysis for the $Z\gamma$ process. The averaged likelihood $L(V_h, \{\mathcal{O}\}; \eta_3, \xi_3)$ is shown in Fig. 6 on log-scale. Here also the dot on the middle of the plot is for unpolarized case while the plus mark at $P_{Z\gamma} = (+0.09, -0.10)$ is for the minimum averaged likelihood and hence the best choice of beam polarizations. The corresponding simultaneous limits on the anomalous couplings h_i is presented in Table 2. Again we notice that the limits obtained for the best choice of beam polarizations $P_{Z\gamma}$ are tighter than any other point on the polarization plane yet comparable to the nearby polarization choices, including the unpolarized case. This again is due to the comparable values of averaged likelihood for $P_{Z\gamma}$ and the unpolarized case. The simultaneous limits for the unpolarized case (also the $P_{Z\gamma}$) turns out to be much better than the ones reported in Ref. [28] for $h_{1,3}^\gamma$ due to the inclusions of new asymmetries in the present analysis. The CP -odd asymmetry \tilde{A}_{yz} has dependence on $h_1^{\gamma,Z}$ with a large sensitivity towards h_1^γ leading to an improvement in the corresponding limit by a factor of two compare to earlier report when adjusted for systematic errors. The limit on h_3^γ improves by a factor of three owing to the asymmetry \tilde{A}_{xz} . The limits on $h_{1,3}^Z$ remains comparable.

The combine analysis of the processes ZZ and $Z\gamma$ is expected to change the best choice of beam polarizations and limits accordingly. For the average likelihood for these two processes the volume, in which one should average,

Table 1 List of simultaneous limits on anomalous couplings obtained for $\sqrt{s} = 500$ GeV and $L = 100 \text{ fb}^{-1}$ for different η_3 and ξ_3 from MCMC in ZZ process.

Beam polarizations	Limits on couplings(10^{-3})								
	f_4^γ		f_4^Z		f_5^γ		f_5^Z		
(η_3, ξ_3)	68%	95%	68%	95%	68%	95%	68%	95%	Comments
$-0.80, +0.80$	+7.3 -9.3	+13.0 -12.0	+15.0 -14.0	+18.0 -19.0	± 7.3	± 13.0	± 11.0	+19.0 -18.0	
$-0.40, +0.40$	± 3.1	+5.8 -5.7	± 4.4	+8.2 -8.4	± 3.3	+6.3 -6.2	+4.5 -5.2	+9.3 -8.5	
$+0.00, +0.00$	± 1.7	± 3.3	± 2.5	± 4.8	± 1.9	+3.7 -3.6	+2.3 -2.7	+5.1 -4.6	
$+0.09, -0.10$	± 1.7	± 3.2	± 2.4	+4.7 -4.6	± 1.8	+3.5 -3.4	+2.2 -2.6	+4.9 -4.5	$P_{Z\gamma}$, best-choice for $Z\gamma$
$+0.12, -0.12$	± 1.6	± 3.1	± 2.4	± 4.7	± 1.8	+3.5 -3.4	+2.2 -2.6	+5.0 -4.5	P_{best} , combined best choice
$+0.16, -0.16$	± 1.6	± 3.1	± 2.4	± 4.7	± 1.8	+3.5 -3.4	+2.3 -2.7	+5.1 -4.5	P_{ZZ} , best-choice for ZZ
$+0.40, -0.40$	± 1.9	± 3.7	± 3.2	+6.1 -6.2	± 2.1	+4.0 -4.1	+3.1 -3.7	+6.7 -6.0	
$+0.80, -0.80$	+5.3 -6.2	+9.8 -9.3	+9.7 -12.0	+18.0 -17.0	± 5.4	+9.5 -9.9	± 9.9	+17.0 -18.0	

Table 2 List of simultaneous limits on anomalous couplings obtained for $\sqrt{s} = 500$ GeV and $L = 100 \text{ fb}^{-1}$ for different η_3 and ξ_3 from MCMC in $Z\gamma$ process.

Beam polarizations	Limits on couplings(10^{-3})								
	h_1^γ		h_1^Z		h_3^γ		h_3^Z		
(η_3, ξ_3)	68%	95%	68%	95%	68%	95%	68%	95%	Comments
$-0.80, +0.80$	$^{+7.7}_{-9.3}$	± 13.0	± 11.0	$^{+18.0}_{-19.0}$	± 7.5	± 13.0	± 11.0	± 19.0	
$-0.40, +0.40$	± 3.9	$^{+7.4}_{-7.5}$	± 6.5	± 12.0	$^{+4.4}_{-3.7}$	$^{+7.1}_{-8.0}$	± 6.6	$^{+13.0}_{-12.0}$	
$+0.00, +0.00$	± 1.6	± 3.1	± 3.7	$^{+7.1}_{-7.0}$	$^{+1.6}_{-1.4}$	$^{+2.8}_{-3.0}$	± 3.6	± 7.1	
$+0.09, -0.10$	± 1.5	± 2.9	± 3.6	± 7.0	$^{+1.4}_{-1.3}$	$^{+2.6}_{-2.8}$	± 3.6	$^{+7.0}_{-7.1}$	$P_{Z\gamma}$, best-choice for $Z\gamma$
$+0.12, -0.12$	± 1.5	± 2.9	± 3.7	± 7.1	± 1.4	$^{+2.6}_{-2.8}$	± 3.6	± 7.1	P_{best} , combined best choice
$+0.16, -0.16$	± 1.5	± 3.0	± 3.7	$^{7.2}_{7.3}$	$^{1.5}_{1.3}$	$^{+2.6}_{-2.8}$	± 3.7	$^{+7.1}_{-7.3}$	P_{ZZ} , best-choice for ZZ
$+0.40, -0.40$	± 2.4	± 4.6	± 5.2	± 10.0	$^{+2.5}_{-2.2}$	$^{+4.3}_{-4.7}$	± 5.2	± 10.0	
$+0.80, -0.80$	± 5.8	$^{+10.0}_{-9.9}$	$^{+11.0}_{-13.0}$	$^{+19.0}_{-18.0}$	$^{+5.8}_{-7.2}$	$^{+10.0}_{-9.7}$	$^{+13.0}_{-15.0}$	$^{+19.0}_{-18.0}$	

will change to $V_{\mathbf{f}/\mathbf{h}} \rightarrow V_{\mathbf{F}}$, where $\mathbf{F} = \{\mathbf{f}, \mathbf{h}\}$ and observables from both the processes should be added to likelihood defined in Eq. 13. The combined averaged likelihood showing dependence on beam polarizations for the two processes considered here is shown in Fig. 7. The dot on the middle of the plot is for unpolarized case and asterisk mark at $P_{best} = (+0.12, -0.12)$ is the combined best choice of beam polarizations. Other points are due to P_{ZZ} and $P_{Z\gamma}$. The combined best choice point sits in between P_{ZZ} and $P_{Z\gamma}$. The limits, presented in Table. 1 and 2, at the combined best choice of beam polarizations are slightly weaker than the limit at the best choice points but comparable in both the process as expected. Thus the combined best choice can be a good

benchmark beam polarizations for the process ZZ and $Z\gamma$ to study at ILC.

Similar analysis can be done by combining many processes, as one should do, to choose a suitable beam polarizations at ILC. For many processes (e.g. we can include WW production with anomalous couplings among charged gauge boson) with different couplings the volume, in which one should do the average, will change to $V_{\mathbf{f}/\mathbf{h}} = V_{\mathbf{F}}$, where \mathbf{F} would be set of all couplings for all the processes considered. The set of observables $\{\mathcal{O}\}$ would include all the relevant observable from all the processes combined in the expression for the likelihood.

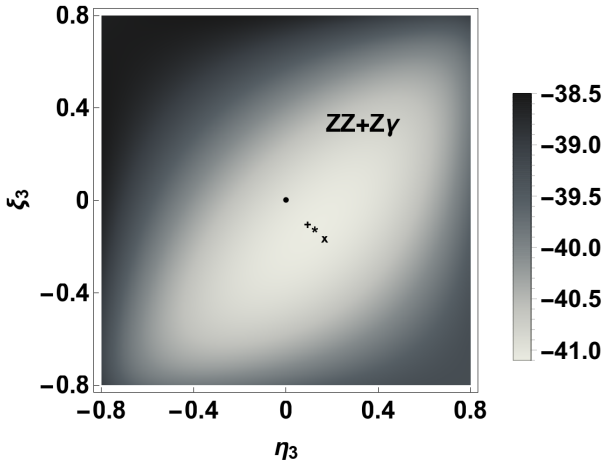


Fig. 7 The log of average likelihood, $\log[L(V_{\{f,h\}}, \{\mathcal{O}\}; \eta_3, \xi_3)]$, is shown considering both the processes ZZ and $Z\gamma$ at $\sqrt{s} = 500$ GeV, $\mathcal{L} = 100 \text{ fb}^{-1}$. The asterisk mark at $P_{\text{best}} = (+0.12, -0.12)$ is the combined best choice for beam polarizations while the other points are for ZZ (cross mark) and $Z\gamma$ (plus mark).

4 Conclusion

To summarize, we aim to find the best choice of beam polarization for an e^+e^- collider to probe the anomalous coupling in the neutral gauge bosons sector in the ZZ and $Z\gamma$ processes. We studied the effects of beam polarization on polarization asymmetries and corresponding sensitivities towards anomalous couplings. Using *minimum averaged* likelihood, we find the best choice of the beam polarization for the two processes and also the combined best choice. Here the list of observables includes the cross-section along with eight polarization asymmetries for the Z boson. Simultaneous limits on anomalous couplings were obtained using MCMC method for a set of benchmark beam polarization including the best choices and they are listed in Tables 1 and 2. The limits obtained for the unpolarized case are better than the ones reported in Ref. [28]. This is because the present analysis includes three new observables \tilde{A}_z , \tilde{A}_{xz} and \tilde{A}_{yz} . These new asymmetries yields better limits on $f_{4,5}^Z$ and $h_{1,3}^Z$ while comparable (yet better) limits on $f_{4,5}^\gamma$ and $h_{1,3}^\gamma$. Comparing the limits for various benchmark beam polarizations from Tables 1 and 2, we find that all three *best* beam polarization choices yield comparable limits and they are comparable to the unpolarized case as well. Thus, as far as anomalous couplings in the neutral gauge boson sector is concerned, unpolarized beams perform as good as the *best* choices. This conclusion, however, can change if one includes more or different set of observables in the analysis or adds more processes to the analysis. For example, processes involving W^\pm or a Higgs boson may have a different preference for the beam polarization.

Considering the physics impact and the cost of beam polarizations at ILC one may chose the unpolarized beams

for the first run, at least for the two processes studied here. But as we infer a detail global analysis is required involving other processes as well to conclude this. We further note that the case of transverse beam polarization is not addressed here and conclusions may differ in that case.

Acknowledgements: R.R. thanks Department of Science and Technology, Government of India for support through DST-INSPIRE Fellowship for doctoral program, INSPIRE CODE IF140075, 2014.

References

1. S. Chatrchyan *et al.* [CMS Collaboration], “Observation of a new boson at a mass of 125 GeV with the CMS experiment at the LHC,” *Phys. Lett. B* **716**, 30 (2012) doi:10.1016/j.physletb.2012.08.021 [arXiv:1207.7235 [hep-ex]].
2. G. Aarons *et al.* [ILC Collaboration], “International Linear Collider Reference Design Report Volume 2: Physics at the ILC,” arXiv:0709.1893 [hep-ph].
3. T. Behnke *et al.*, “The International Linear Collider Technical Design Report - Volume 1: Executive Summary,” arXiv:1306.6327 [physics.acc-ph].
4. H. Baer *et al.*, “The International Linear Collider Technical Design Report - Volume 2: Physics,” arXiv:1306.6352 [hep-ph].
5. G. Moortgat-Pick *et al.*, “The Role of polarized positrons and electrons in revealing fundamental interactions at the linear collider,” *Phys. Rept.* **460**, 131 (2008) doi:10.1016/j.physrep.2007.12.003 [hep-ph/0507011].
6. V. V. Andreev, G. Moortgat-Pick, P. Osland, A. A. Pankov and N. Paver, “Discriminating Z' from Anomalous Trilinear Gauge Coupling Signatures in $e^+e^- \rightarrow W^+W^-$ at ILC with Polarized Beams,” *Eur. Phys. J. C* **72**, 2147 (2012) doi:10.1140/epjc/s10052-012-2147-2 [arXiv:1205.0866 [hep-ph]].
7. B. Ananthanarayan, M. Patra and P. Poullose, “Signals of additional Z boson in $e^+e^- \rightarrow W^+W^-$ at the ILC with polarized beams,” *JHEP* **1102**, 043 (2011) doi:10.1007/JHEP02(2011)043 [arXiv:1012.3566 [hep-ph]].
8. P. Osland, A. A. Pankov and A. V. Tsytrinov, “Identification of extra neutral gauge bosons at the International Linear Collider,” *Eur. Phys. J. C* **67**, 191 (2010) doi:10.1140/epjc/s10052-010-1272-z [arXiv:0912.2806 [hep-ph]].
9. A. A. Pankov, N. Paver and A. V. Tsytrinov, “Distinguishing new physics scenarios at a linear collider with polarized beams,” *Phys. Rev. D* **73**, 115005 (2006) doi:10.1103/PhysRevD.73.115005 [hep-ph/0512131].
10. O. Kittel, G. Moortgat-Pick, K. Rolbiecki, P. Schade and M. Terwort, “Measurement of CP asymmetries

- in neutralino production at the ILC,” *Eur. Phys. J. C* **72**, 1854 (2012) doi:10.1140/epjc/s10052-011-1854-4 [arXiv:1108.3220 [hep-ph]].
11. H. K. Dreiner, O. Kittel and A. Marold, “Normal tau polarisation as a sensitive probe of CP violation in chargino decay,” *Phys. Rev. D* **82**, 116005 (2010) doi:10.1103/PhysRevD.82.116005 [arXiv:1001.4714 [hep-ph]].
 12. A. Bartl, K. Hohenwarter-Sodek, T. Kernreiter and O. Kittel, “CP asymmetries with longitudinal and transverse beam polarizations in neutralino production and decay into the Z0 boson at the ILC,” *JHEP* **0709**, 079 (2007) doi:10.1088/1126-6708/2007/09/079 [arXiv:0706.3822 [hep-ph]].
 13. K. Rao and S. D. Rindani, “Probing CP-violating contact interactions in $e^+e^- \rightarrow HZ$ with polarized beams,” *Phys. Lett. B* **642**, 85 (2006) doi:10.1016/j.physletb.2006.07.072 [hep-ph/0605298].
 14. A. Bartl, H. Fraas, S. Hesselbach, K. Hohenwarter-Sodek, T. Kernreiter and G. A. Moortgat-Pick, “CP-odd observables in neutralino production with transverse e^+ and e^- beam polarization,” *JHEP* **0601**, 170 (2006) doi:10.1088/1126-6708/2006/01/170 [hep-ph/0510029].
 15. H. Czyz, K. Kolodziej and M. Zralek, “Composite Z Boson and CP Violation in the Process $e^+e^- \rightarrow Z\gamma$,” *Z. Phys. C* **43**, 97 (1989). doi:10.1007/BF02430614
 16. D. Choudhury and S. D. Rindani, “Test of CP violating neutral gauge boson vertices in $e^+e^- \rightarrow \gamma Z$,” *Phys. Lett. B* **335**, 198 (1994) doi:10.1016/0370-2693(94)91413-3 [hep-ph/9405242].
 17. B. Ananthanarayan, S. D. Rindani, R. K. Singh and A. Bartl, “Transverse beam polarization and CP-violating triple-gauge-boson couplings in $e^+e^- \rightarrow \gamma Z$,” *Phys. Lett. B* **593**, 95 (2004) Erratum: [*Phys. Lett. B* **608**, 274 (2005)] doi:10.1016/j.physletb.2004.04.067, 10.1016/j.physletb.2005.01.009 [hep-ph/0404106].
 18. B. Ananthanarayan, S. K. Garg, M. Patra and S. D. Rindani, “Isolating CP-violating γZZ coupling in $e^+e^- \rightarrow \gamma Z$ with transverse beam polarizations,” *Phys. Rev. D* **85**, 034006 (2012) doi:10.1103/PhysRevD.85.034006 [arXiv:1104.3645 [hep-ph]].
 19. B. Ananthanarayan and S. D. Rindani, “CP violation at a linear collider with transverse polarization,” *Phys. Rev. D* **70**, 036005 (2004) doi:10.1103/PhysRevD.70.036005 [hep-ph/0309260].
 20. S. Groote, J. G. Korner, B. Melic and S. Prelovsek, “A survey of top quark polarization at a polarized linear e^+e^- collider,” *Phys. Rev. D* **83**, 054018 (2011) doi:10.1103/PhysRevD.83.054018 [arXiv:1012.4600 [hep-ph]].
 21. M. S. Amjad *et al.*, “A precise characterisation of the top quark electro-weak vertices at the ILC,” *Eur. Phys. J. C* **75**, no. 10, 512 (2015) doi:10.1140/epjc/s10052-015-3746-5 [arXiv:1505.06020 [hep-ex]].
 22. B. Ananthanarayan, M. Patra and P. Poullose, “W physics at the ILC with polarized beams as a probe of the Littlest Higgs Model,” *JHEP* **0911**, 058 (2009) doi:10.1088/1126-6708/2009/11/058 [arXiv:0909.5323 [hep-ph]].
 23. B. Ananthanarayan, M. Patra and P. Poullose, “Probing strongly interacting W’s at the ILC with polarized beams,” *JHEP* **1203**, 060 (2012) doi:10.1007/JHEP03(2012)060 [arXiv:1112.5020 [hep-ph]].
 24. S. Kumar, P. Poullose and S. Sahoo, “Study of Higgs-gauge boson anomalous couplings through $e^-e^+ \rightarrow W^-W^+H$ at ILC,” *Phys. Rev. D* **91**, no. 7, 073016 (2015) doi:10.1103/PhysRevD.91.073016 [arXiv:1501.03283 [hep-ph]].
 25. S. D. Rindani and P. Sharma, “Decay-lepton correlations as probes of anomalous ZZH and γZH interactions in $e^+e^- \rightarrow ZH$ with polarized beams,” *Phys. Lett. B* **693**, 134 (2010) doi:10.1016/j.physletb.2010.08.027 [arXiv:1001.4931 [hep-ph]].
 26. S. S. Biswal and R. M. Godbole, “Use of transverse beam polarization to probe anomalous VVH interactions at a Linear Collider,” *Phys. Lett. B* **680**, 81 (2009) doi:10.1016/j.physletb.2009.08.014 [arXiv:0906.5471 [hep-ph]].
 27. S. D. Rindani and P. Sharma, “Angular distributions as a probe of anomalous ZZH and γZH interactions at a linear collider with polarized beams,” *Phys. Rev. D* **79**, 075007 (2009) doi:10.1103/PhysRevD.79.075007 [arXiv:0901.2821 [hep-ph]].
 28. R. Rahaman and R. K. Singh, “On polarization parameters of spin-1 particles and anomalous couplings in $e^+e^- \rightarrow ZZ/Z\gamma$,” *Eur. Phys. J. C* **76**, no. 10, 539 (2016) doi:10.1140/epjc/s10052-016-4374-4 [arXiv:1604.06677 [hep-ph]].
 29. F. Boudjema and R. K. Singh, “A Model independent spin analysis of fundamental particles using azimuthal asymmetries,” *JHEP* **0907**, 028 (2009) arXiv:0903.4705 [hep-ph].
 30. J. A. Aguilar-Saavedra and J. Bernabeu, “Breaking down the entire W boson spin observables from its decay,” *Phys. Rev. D* **93**, no. 1, 011301 (2016) doi:10.1103/PhysRevD.93.011301 [arXiv:1508.04592 [hep-ph]].
 31. F. Boudjema, *Proc. of the Workshop on e^-e^+ Collisions at 500GeV: The Physics Potential*, DESY 92-123B (1992) p.757, edited by P.M. Zerwas.
 32. U. Baur and E. L. Berger, “Probing the weak boson sector in $Z\gamma$ production at hadron colliders,” *Phys. Rev. D* **47**, 4889 (1993). doi:10.1103/PhysRevD.47.4889

33. J. Ellison and J. Wudka, “Study of trilinear gauge boson couplings at the Tevatron collider,” *Ann. Rev. Nucl. Part. Sci.* **48**, 33 (1998) doi:10.1146/annurev.nucl.48.1.33 [hep-ph/9804322].
34. U. Baur and D. L. Rainwater, “Probing neutral gauge boson selfinteractions in ZZ production at hadron colliders,” *Phys. Rev. D* **62**, 113011 (2000) doi:10.1103/PhysRevD.62.113011 [hep-ph/0008063].
35. H. Aihara *et al.*, “Anomalous gauge boson interactions,” In *Barklow, T.L. (ed.) et al.: Electroweak symmetry breaking and new physics at the TeV scale* 488-546 doi:10.1142/97898128302650009 [hep-ph/9503425].
36. B. Ananthanarayan and S. D. Rindani, “New physics in $e^+e^- \rightarrow Z\gamma$ with polarized beams,” *JHEP* **0510**, 077 (2005) doi:10.1088/1126-6708/2005/10/077 [hep-ph/0507037].
37. G. J. Gounaris, J. Layssac and F. M. Renard, “Off-shell structure of the anomalous Z and γ selfcouplings,” *Phys. Rev. D* **62**, 073012 (2000) doi:10.1103/PhysRevD.62.073012 [hep-ph/0005269].
38. P. Poulose and S. D. Rindani, “CP violating $Z\gamma\gamma$ and top quark electric dipole couplings in $\gamma\gamma \rightarrow t\bar{t}$,” *Phys. Lett. B* **452**, 347 (1999) doi:10.1016/S0370-2693(99)00236-1 [hep-ph/9809203].
39. I. Ots, H. Uiho, H. Liivat, R. Saar and R. K. Loide, “Possible anomalous ZZ gamma and Z gamma gamma couplings and Z boson spin orientation in $e^+e^- \rightarrow Z\gamma$: The role of transverse polarization,” *Nucl. Phys. B* **740**, 212 (2006). doi:10.1016/j.nuclphysb.2006.02.003
40. G. J. Gounaris, J. Layssac and F. M. Renard, “Signatures of the anomalous $Z\gamma$ and ZZ production at the lepton and hadron colliders,” *Phys. Rev. D* **61**, 073013 (2000) doi:10.1103/PhysRevD.61.073013 [hep-ph/9910395].
41. S. Y. Choi, “Probing the weak boson sector in $\gamma e \rightarrow Ze$,” *Z. Phys. C* **68**, 163 (1995) doi:10.1007/BF01579815 [hep-ph/9412300].
42. T. G. Rizzo, “Polarization asymmetries in gamma e collisions and triple gauge boson couplings revisited,” hep-ph/9907395, hep-ph/9907395.
43. S. Atag and I. Sahin, “ZZ gamma and Z gamma gamma couplings in gamma e collision with polarized beams,” *Phys. Rev. D* **68**, 093014 (2003) doi:10.1103/PhysRevD.68.093014 [hep-ph/0310047].
44. B. Ananthanarayan, J. Lahiri, M. Patra and S. D. Rindani, “New physics in $e^+e^- \rightarrow Z\gamma$ at the ILC with polarized beams: explorations beyond conventional anomalous triple gauge boson couplings,” *JHEP* **1408**, 124 (2014) doi:10.1007/JHEP08(2014)124 [arXiv:1404.4845 [hep-ph]].
45. V. Khachatryan *et al.* [CMS Collaboration], “Measurements of the ZZ production cross sections in the $2l2\nu$ channel in protonproton collisions at $\sqrt{s} = 7$ and 8 TeV and combined constraints on triple gauge couplings,” *Eur. Phys. J. C* **75**, no. 10, 511 (2015) doi:10.1140/epjc/s10052-015-3706-0 [arXiv:1503.05467 [hep-ex]].
46. G. Aad *et al.* [ATLAS Collaboration], “Measurements of $Z\gamma$ and $Z\gamma\gamma$ production in pp collisions at $\sqrt{s} = 8$ TeV with the ATLAS detector,” *Phys. Rev. D* **93**, no. 11, 112002 (2016) doi:10.1103/PhysRevD.93.112002 [arXiv:1604.05232 [hep-ex]].